

Biological Trace Element Research

Synthesis and Biodistribution Study of Biocompatible ¹⁹⁸Au Nanoparticles by use of Arabinoxylan as Reducing and Stabilizing Agent --Manuscript Draft--

Manuscript Number:	BTER-D-18-01156R3
Full Title:	Synthesis and Biodistribution Study of Biocompatible ¹⁹⁸ Au Nanoparticles by use of Arabinoxylan as Reducing and Stabilizing Agent
Article Type:	Original Article
Keywords:	Hemicelluloses; Arabinoxylan; Gold nanoparticles; Targeted delivery; Radioactive gold nanoparticles
Corresponding Author:	Mohammad S. Iqbal, PhD Forman Christian College Lahore, Punjab PAKISTAN
Corresponding Author Secondary Information:	
Corresponding Author's Institution:	Forman Christian College
Corresponding Author's Secondary Institution:	
First Author:	Fozia Iram, PhD
First Author Secondary Information:	
Order of Authors:	Fozia Iram, PhD Mohammad S. Iqbal, PhD Irfan Ullah Khan, PhD Rashid Rasheed, MS Aqsa Khalid, BS Muhammad Khalid, PhD Saira Aftab, MS Abdul R Shakoori, PhD
Order of Authors Secondary Information:	
Funding Information:	
Abstract:	<p>Radioactive gold-198 is a useful diagnostic and therapeutic agent. Gold in the form of nanoparticles possesses even more exciting properties. This work aimed at arabinoxylan-mediated synthesis and biodistribution study of radioactive gold nanoparticles (¹⁹⁸AuNPs). The particles were synthesized by mixing suspension of arabinoxylan with H¹⁹⁸AuCl₄ without use of any additional reducing and stabilizing agents. An aqueous suspension of arabinoxylan was added to a H¹⁹⁸AuCl₄ solution, which resulted in reduction of Au³⁺ to ¹⁹⁸AuNPs. Biodistribution was studied in vitro and in rabbit. The particles having exceptional stability were readily formed. Highest radioactivity was recorded in spleen after 3 h followed by liver, heart, kidney and lungs after i.v. administration. After 24 h the activity was not detectable in spleen; it accumulated in liver. However, after oral administration the activity mainly accumulated in colon. In serum proteins the distribution was: α₁-globulin 6.5%, α₂-globulin ~2%, β-globulin ~1%, γ-globulin 0.7% and albumin 0.7% of the administered dose. This indicates a low protein binding implying high bioavailability of the particles. The cytotoxicity study showed that the particles were inactive against HeLa cell line and A. tumefaciens. Highly stable ¹⁹⁸AuNPs reported in this work have potential for targeting colon. They show affinity for globulins, the property that can be used in study of immune system.</p>

The Editor
BTER

Dec 30, 2018

Dear Sir,

I am submitting a research paper "Synthesis and Biodistribution Study of Biocompatible ^{198}Au Nanoparticles by use of Arabinoxylan as Reducing and Stabilizing Agent" for publication in BTER. This has the approval of all the authors. The work describes synthesis of radioactive gold nanoparticles by use of arabinoxylan – biomaterial isolated from from ispaghula (*Plantago ovata*) husk. The particles are non-toxic, free from hazardous reducing and capping agents and exhibit potential for imaging and diagnosis.

The paper is solely being submitted to this journal. This work does not involve any conflict of interest. Valid institutional email address or ORCID ID of each author is given below.

Fozia Iram ORCID ID: 0000-0001-7252-2164	Aqsa Khalid ORCID ID: 0000-0002-8504-2992
Mohammad S Iqbal ORCID ID: 0000-0002-2933-195X	Muhammad Khalid E-mail: mkhalid@pinstech.org.pk
Irfan U Khan ORCID ID: 0000-0002-8348-3807	Saira Aftab E-mail: saira.sbs@pu.edu.pk
Rashid Rasheed ORCID ID: 0000-0002-5447-1831	Abdul R Shakoori E-mail: arshakoori.sbs@pu.edu.pk

Thanks and regards.



Mohammad S Iqbal, PhD
Professor
Department of Chemistry
Forman Christian College
Lahore, Pakistan.
Phone: 92-300-4262813
E-mail: saeediq50@hotmail.com; saeediqbal@fccollege.edu.pk

Response to reviewer's comments

The responses are in **red** in the manuscript and in here.

Reviewer 2

Comment

The authors still need to provide a statistics section in the materials and methods. The authors added info on N and P values in the figure legends but provided no information about statistical methods or software used to analyze the data (e.g. T tests, ANOVA, etc).

Response

The section "**Statistical Analysis**" has been added at page 13 as the last paragraph in "**Materials and Methods**".

1
2
3
4
5
6
7
8
9
10
11
12
13
14
15
16
17
18
19
20
21
22
23
24
25
26
27
28
29
30
31
32
33
34
35
36
37
38
39
40
41
42
43
44
45
46
47
48
49
50
51
52
53
54
55
56
57
58
59
60
61
62
63
64
65

Synthesis and Biodistribution Study of Biocompatible ^{198}Au Nanoparticles by use of Arabinoxylan as Reducing and Stabilizing Agent

Fozia Iram

Department of Chemistry, LCW University, Lahore 54600, Pakistan.

E-mail: fozia_iram@hotmail.com, Phone: 92 333 8231615

Mohammad S Iqbal*

Department of Chemistry, Forman Christian College, Lahore 54600, Pakistan.

E-mail : saeediq50@hotmail.com, Phone: 92 300 4262813

Irfan U Khan

Radiopharmacy & PET Radiochemistry Division, Institute of Nuclear Medicine and Oncology,

Lahore. E-mail: drirfankhan69@gmail.com, Phone: 92 3224110569

Rashid Rasheed

Institute of Nuclear Medicine Oncology and Radiotherapy, Mansehra Road, Abbottabad,

Pakistan. E-mail: dr.nmd.paec@gmail.com, Phone: 92 3336523396

Aqsa Khalid

Department of Chemistry, LCW University, Lahore 54600, Pakistan.

E-mail: aqsa.aslam92@gmail.com, Phone: 92 3016227013

Muhammad Khalid

Isotope Production Division, Pakistan Institute of Nuclear Science and Technology, PO Nilore,

Islamabad, Pakistan. E-mail: mkhalid@pinstech.org.pk. Phone: 92 3320743333

Saira Aftab

School of Biological Sciences, University of the Punjab, Quaid-e-Azam Campus, Lahore 54590,

Pakistan. E-mail:sairaftab@gmail.com, Phone: 92 3216205182

Abdul R Shakoori

School of Biological Sciences, University of the Punjab, Quaid-e-Azam Campus, Lahore 54590,

Pakistan. E-mail: drali1978@gmail.com, Phone: 92 3334533964

*Corresponding author. Tel.: +92 300 4262813.

E-mail address: saeediq50@hotmail.com (M.S. Iqbal)

1
2
3
4
5
6
7
8 **Synthesis and Biodistribution Study of Biocompatible ¹⁹⁸Au**
9
10 **Nanoparticles by use of Arabinoxylan as Reducing and Stabilizing**
11 **agent**
12
13

14 Fozia Iram¹ • Mohammad S Iqbal^{2*} • Irfan U Khan³ • Rashid Rasheed⁴ • Aqsa Khalid¹ •
15 Muhammad Khalid⁵ • Saira Aftab⁶ • Abdul R Shakoori⁶
16
17
18
19

20 ¹Department of Chemistry, LCW University, Lahore 54600, Pakistan

21 ²Department of Chemistry, Forman Christian College, Lahore 54600, Pakistan

22 ³Radiopharmacy & PET Radiochemistry Division, Institute of Nuclear Medicine and Oncology
23 Lahore, Pakistan

24 ⁴Institute of Nuclear Medicine Oncology and Radiotherapy, Abbottabad, Pakistan

25 ⁵Isotope Production Division, Pakistan Institute of Nuclear Science and Technology PO Nilore,
26 Islamabad, Pakistan

27 ⁶School of Biological Sciences, University of the Punjab, Quaid-e-Azam Campus, Lahore 54590,
28 Pakistan
29
30
31

32 **Abstract**

33 Radioactive gold-198 is a useful diagnostic and therapeutic agent. Gold in the form of
34 nanoparticles possesses even more exciting properties. This work aimed at arabinoxylan-
35 mediated synthesis and biodistribution study of radioactive gold nanoparticles (¹⁹⁸AuNPs). The
36 particles were synthesized by mixing suspension of arabinoxylan with H¹⁹⁸AuCl₄ without use of
37 any additional reducing and stabilizing agents. An aqueous suspension of arabinoxylan was
38 added to a H¹⁹⁸AuCl₄ solution, which resulted in reduction of Au³⁺ to ¹⁹⁸AuNPs. Biodistribution
39 was studied *in vitro* and in rabbit. The particles having exceptional stability were readily formed.
40 Highest radioactivity was recorded in spleen after 3 h followed by liver, heart, kidney and lungs
41 after *i.v.* administration. After 24 h the activity was not detectable in spleen; it accumulated in
42 liver. However, after oral administration the activity mainly accumulated in colon. In serum
43 proteins the distribution was: α₁-globulin 6.5%, α₂-globulin ~2%, β-globulin ~1%, γ-globulin
44 0.7% and albumin 0.7% of the administered dose. This indicates a low protein binding implying
45 high bioavailability of the particles. The cytotoxicity study showed that the particles were
46 inactive against HeLa cell line and *A. tumefaciens*. Highly stable ¹⁹⁸AuNPs reported in this work
47 have potential for targeting colon. They show affinity for globulins, the property that can used in
48 study of immune system.
49
50
51
52
53

54 **Keywords** Hemicelluloses • Arabinoxylan • Gold nanoparticles • Targeted delivery •
55 Radioactive gold nanoparticles
56
57

58 *Corresponding author. Tel.: +92 300 4262813.

59 E-mail address: saeediq50@hotmail.com (M.S. Iqbal)
60
61
62
63
64
65

Introduction

AuNPs are being widely studied for their potential applications in therapy, diagnosis, drug delivery and imaging due to their unique properties such as inertness, ease of synthesis, functionalizability and peculiar optical properties [1–8]. The efficiency of NPs in biomedical imaging largely depends on their optical properties. The size dependent optical properties of AuNPs, including linear surface plasmon resonance, fluorescence and Raman scattering, make them ideal candidate for organ imaging and optical sensors [9–11]. The particles having size 3 – 40 nm absorb at 510 – 530 nm with extinction coefficients to the order of $10^{11} \text{ mol}^{-1} \text{ cm}^{-1}$, that is much higher than those of conventional dyes used for imaging. In case of particles > 40 nm the scattering-to-absorption ratio is several orders higher than those of fluorescent dyes [12, 13]. On account of these properties AuNPs have been widely investigated for diagnostic imaging [4, 14]. AuNPs have also been investigated for their use in photothermal destruction of cancerous cells due to their excellent thermal conductivity [1, 15, 16].

In the present work we hypothesize that AuNPs encapsulated in arabinoxylan (AX), a swellable hemicellulosic material, would exhibit organ specific uptake and if the gold is radioactive they can be used for radioimaging. ^{198}Au is a radioactive isotope of gold that emits β -particles and γ -rays of energies 0.412, 0.68 and 1.09 MeV. The γ -radiation of 0.412 MeV energy is highly suitable for imaging human organs. On the other hand β -particles have been successfully employed for treating prostate tumours [17–25].

Generally AuNPs are synthesized by chemical methods involving use of highly toxic reducing agents such as sodium borohydride, hydrazine or formaldehyde [26–28] and capped with stabilizing agents. Although the particles are thoroughly washed but the process does not rule out the presence of residual amount of the toxic reducing agents. For biomedical

1
2
3
4 applications the particles need to be absolutely free from toxic materials. In order to ensure this
5
6 the use of toxic materials in the synthesis of NPs has to be eliminated. Recently, highly
7
8 biocompatible and biodegradable materials have been identified as reducing and stabilizing
9
10 agents. These include hemicelluloses, which can simultaneously reduce Au³⁺ to Au⁰ and stabilize
11
12 them for more than three years [29, 30].
13
14

15
16 In the present study we have used AX from ispaghula (*Plantago ovata*) husk for the
17
18 synthesis and stabilization of radioactive ¹⁹⁸AuNPs coupled with their biodistribution *in vitro* and
19
20 *in vivo*. AX has the potential to deliver encapsulated drugs at colon as this material is insoluble in
21
22 acidic and soluble in alkaline media [31]. Thus when administered orally the AX-encapsulated
23
24 AuNPs are expected to remain intact in stomach (pH < 2) and pass onto intestine where they get
25
26 dissolved and hydrolyzed due to alkaline pH and the presence of micro flora there [32]. They are
27
28 not digested in the small intestine and can easily pass to colon where they can be partially
29
30 digested and release encapsulated particles. Moreover, the hydrophilic nature of AX and its high
31
32 affinity toward mucosal surfaces would assist the encapsulated particles to be released for longer
33
34 periods of time at the specific site [33]. Thus we hypothesize that AX-encapsulated ¹⁹⁸AuNPs are
35
36 biocompatible and suitable for diagnosis and therapy of colon related malignancies.
37
38
39
40
41
42
43
44

45 **Materials and Methods**

46 **Materials**

47
48
49
50
51
52
53 The materials used in this study were: gold (ARY Gold, Lahore, 99.99%), NaOH, HNO₃ and
54
55 HCl, Extrapure[®] from E. Merck, Germany; L-(+)-arabinose, D-(+)-galactose, D-glucose, D-(+)-
56
57 xylose, L-rhamnose monohydrate, galacturonic acid, Citric acid, from E. Merck, Germany;
58
59
60
61
62
63
64
65

1
2
3
4 oligosaccharides β -(1-4)-D-xylotriose, β -(1-4)-D-xylotetraose, β -(1-4)-D-xylopentaose, and β -(1-
5
6 4)-D-xylohexaose used as GPC standards were from Megazyme (Sydney, Australia); reactant
7
8 free AuNPs (30 nm) stabilized in phosphate buffer, Coomassie Brilliant Blue R-250, dimethyl
9
10 sulfoxide (DMSO), glycerol, bovine serum albumin (BSA), human serum albumin (HSA),
11
12 neutral red, glacial acetic acid, *l*-cysteine, disodium hydrogen phosphate, sodium nitrate and
13
14 sodium dodecyl sulfate (SDS), were of analytical grade from sigma Aldrich (USA); *A.*
15
16
17 *tumefaciens*, HeLa cells (ATCC: CCL 2) from Flow Labs (London, UK); Dulbecco's Modified
18
19 Eagle Medium (DMEM), fetal bovine serum (FBS) from Gibco (USA); complement protein C₃
20
21 kit was from Orion Diagnostica (Finland). AX (molar mass 3.17×10^6 Da) was a gift from Dr.
22
23 Shazma Massey of FC College Lahore, isolated according to the reported method [34]. The AX
24
25 sample was recharacterized by elemental analysis, monosaccharide composition, ATR-FT-IR
26
27 and gel permeation chromatography (GPC). Nanopure[®] water was used throughout this work. All
28
29 the chemicals were used without further purification.
30
31
32
33
34
35
36
37

38 **Preparation of H¹⁹⁸AuCl₄·3H₂O**

39
40
41
42
43 The gold foil (0.050 g) was irradiated with a neutron flux of 8×10^{13} n·cm²·s⁻¹ for 30 min at the
44
45 research reactor of Pakistan Institute of Nuclear Science and Technology, Islamabad. The
46
47 irradiated gold was dissolved in aqua regia (150 μ L) at 100 °C, evaporated near to dryness,
48
49 followed by addition of HCl (0.01 M) and evaporation near to dryness. The evaporation process
50
51 was repeated three times and the remaining mass was left at room temperature for crystallization
52
53 of H¹⁹⁸AuCl₄·3H₂O.
54
55
56
57
58
59
60
61
62
63
64
65

Synthesis of $^{198}\text{AuNPs}$

The $^{198}\text{AuNPs}$ were synthesized as reported earlier for non-radioactive AuNPs [29]. Briefly, $\text{H}^{198}\text{AuCl}_4 \cdot 3\text{H}_2\text{O}$ (0.0393 g, 0.1 mmol) was dissolved in water (100 mL); to 20 mL of this solution 20 mL of AX-suspension (0.1 % in water) was added under vigorous stirring for 2 h at 50 °C. A successive change in color from pale yellow to red was observed in 25 min, indicating the formation of $^{198}\text{AuNPs}$, however the stirring was continued for further 2 h to ensure complete reduction. The particles were isolated by centrifugation at 35000 rpm for 30 min, re-dispersed in water using an ultrasonic bath, washed with water, centrifuged again and dialyzed to free them from unreacted materials.

Characterization

The AX sample used in this work was recharacterized according to the reported methods [34]. Elemental analysis was carried out by CHNS analyzer (Vario MICRO V1.4.2; Elementar Analysen Systeme, GmbH, Germany). Monosaccharide composition was determined by HPLC using Dionex ICS 3000 system, consisting of CarboPacPA20 column (0.4×150 mm) and electrochemical detector, according to a reported method [35] after acid hydrolysis [36]. ATR-FT-IR spectrum was recorded by Cary 630 FTIR Spectrometer (Agilent, USA). GPC was performed by Agilent 1200 series (Agilent, Germany) system using PL aquagel-OH mixed column (8 μm ; 7.5×300 mm) and refractive index detector (G1362A). Water containing 0.1% NaNO_3 was used as eluent (flow rate: 1.0 mL min^{-1} at 70 °C) and injection volume was 10 mL.

1
2
3
4 Data were analyzed by the Chem-Station GPC Data Analysis Rev. A.02.02 (Agilent, Germany).
5
6

7 Pullulan and dextran were used as calibration standards.
8

9 The AX-encapsulated $^{198}\text{AuNPs}$ samples were diluted four times with water, filtered through
10 0.22 μm membrane and SPR spectra recorded on Pharmaspec UV-1700 spectrophotometer
11 (Shimadzu, Japan) in 300–800 nm range using AX suspension as the reference. The SPR
12 absorption at 526 nm was used to determine the particle size and concentration of Au was
13 determined by using molar absorptivity value of 3.36×10^9 at 526 nm [37]. Stability of the
14 particles was studied in human serum by recording SPR spectra 1 h, 2 h, 48 h and 60 h after
15 appropriate dilution with water.
16
17
18
19
20
21
22
23
24

25 The pXRD spectra of AX-encapsulated $^{198}\text{AuNPs}$ were recorded on Bruker D8 Discover
26 (Germany) diffractometer using monochromatic Cu $K\alpha$ radiation ($\lambda = 1.5406\text{\AA}$) operating at 40
27 kV and 30 mA. The data were collected over a 10–80° 2θ range. The size of particles was
28 calculated from the highest intensity peak in the XRD spectra by use of Debye–Scherrer equation
29 ($D = 0.9\lambda/\beta\cos \theta$) [38].
30
31
32
33
34
35
36
37

38 For transmission electron microscopy (TEM) an ultrasonically dispersed solution of the
39 NPs was placed on a carbon coated grid and images were obtained by JEM-1200EX (JEOL,
40 Japan) microscope at an accelerating voltage of 120 kV.
41
42
43
44
45
46
47

48 **Particle Size Distribution and Zeta Potential**

49
50
51
52

53 Particle size and zeta potential were determined by NanoZS90 HPPS 5001 zetasizer (Malvern,
54 UK). The disposable cuvette was filled with the sample and allowed to equilibrate for 2-3 min at
55
56
57
58
59
60
61
62
63
64
65

1
2
3
4 21°C before the measurement. Ten replicates of each sample were measured and an average
5
6 value was reported.
7

8
9 For zeta potential (ζ) measurements the capillary cell (DTS 1060) was flushed with water
10 and filled with sample avoiding air bubbles in the capillary. Ten replicates were measured and
11 the average values were reported.
12
13
14
15
16
17
18

19 **Cell Viability and Cytotoxicity**

20
21
22

23
24 Cytotoxicity of the AX-encapsulated $^{198}\text{AuNPs}$ was determined by Neutral Red (NR) [39] and
25 potato disc assays [40]. Briefly, HeLa cells were cultured as monolayers into 96-wells plate,
26 containing approximately 1×10^4 cells in each well, DMEM culture medium supplemented with
27 10 % of FBS, glucose (4.500 g L^{-1}) and 1 % of penicillin-streptomycin. The plate was incubated
28 at 37 °C for 24 h under 5% CO_2 and 90% humidity. To the cultured cells, three blanks (one
29 excluding the AX and $^{198}\text{AuNPs}$, the other containing AX ($6.70 \mu\text{g mL}^{-1}$) and excluding
30 $^{198}\text{AuNPs}$), third one excluding AX and containing $^{198}\text{AuNP}$ ($18.0 \mu\text{g mL}^{-1}$) and varying
31 concentrations of AX-encapsulated $^{198}\text{AuNPs}$ ($18.0, 9.0$ and $4.5 \mu\text{g mL}^{-1}$) were added in 1:1 ratio
32 and the plate was incubated again for 24 h under similar conditions. After incubation the medium
33 was drained, cells washed with PBS, the NR dye added and the plate incubated for further 2 h.
34
35 The surplus NR was washed out by freshly prepared de-staining solution (glacial acetic acid-
36 ethanol-water, 1:49: 50) and the culture was incubated for further 10 min. The optical density of
37 the released NR dye was measured at 570 nm. Relative cell viability was calculated as:
38
39
40
41
42
43
44
45
46
47
48
49
50
51
52
53
54
55
56

$$57 \text{ Cell viability (\%)} = \frac{\text{sample absorbance}}{\text{control absorbance}} \times 100$$

58
59
60

1
2
3
4
5
6
7 The potato disc method was also used to assess the cytotoxicity of ¹⁹⁸AuNPs. For this *A.*
8
9 *tumefaciens* was grown on Luria broth medium for 48h at 28°C in shaking incubator. Various
10
11 concentrations of ¹⁹⁸AuNPs (1.8, 9.0 and 4.5 µg mL⁻¹) and of AX suspension (67.0 µg mL⁻¹ were
12
13 tested. Inoculum was prepared by mixing each dilution (100 µL) with bacterial culture (100 µL).
14
15 Negative control was prepared by mixing of water (100 µL) and *A. tumefaciens* (100 µL).
16
17 Roxithromycin (100 ppm: 100 µL) was used as positive control. Red-skinned potatoes were
18
19 purchased from a local market and surface sterilized by using 10 % bleach solution. Cylinders of
20
21 surface sterilized red skinned potato were made with the help of sterilized borer. The 5 mm thick
22
23 discs of these potato cylinders were cut and placed on solidified agar plates (10 discs per plate).
24
25 Inoculum (50 µL) was poured on the surface of each disc of respective concentration as well as
26
27 controls. The discs were examined after 21 days of incubation under dissecting microscope after
28
29 staining with Lugol's solution (potassium iodide-iodine-distilled water in 10:5:7 ratio). The
30
31 number of tumours per disc was counted. The doses for the cytotoxicity tests were chosen by
32
33 considering the radioactivity suitable for imaging. Percentage inhibition for each concentration
34
35 was determined by using the following formula.
36
37
38
39
40
41
42
43
44
45

$$\% \text{ Inhibition} = \frac{\text{No of tumour with sample}}{\text{No of tumour with control}} \times 100$$

46 47 48 49 50 51 52 53 **Biodistribution Studies** 54 55 56 57 58 59 60 61 62 63 64 65

1
2
3
4 Biodistribution experiments were planned to be carried out *in vivo* after intravenous and oral
5
6 administration to healthy rabbits, in tumour-bearing mouse, and *in vitro* among serum proteins as
7
8 follows.
9

10 **Biodistribution after Intravenous Administration of $^{198}\text{AuNPs}$ in Rabbit**

11
12
13
14
15
16
17
18
19 These experiments were conducted at Institute of Nuclear Medicine and Oncology hospital,
20
21 Lahore. The AX suspension containing $^{198}\text{AuNPs}$ equivalent to $14.0 \mu\text{g mL}^{-1}$ Au having ~ 1000
22
23 $\mu\text{Ci mL}^{-1}$ activity was prepared by appropriately diluting the stock suspension. The dose (0.5
24
25 mL), adjusted to pH 7 by use of HCl (0.1 M) or NaOH (0.1 M) solutions, was filtered through
26
27 0.22- μm membrane (Polycarbonate, Sterlitech, USA) and injected into the ear vein of healthy
28
29 rabbits (n = 4; local breed, age 12-16 weeks, average weight 900 ± 50 g). The animals were
30
31 anesthetized by intramuscular ketamine injection (50 mg kg^{-1}) before administration of the dose.
32
33
34 The administered dose was determined by subtracting the activity remaining in the syringe from
35
36 the total taken in the syringe.
37
38
39

40
41 Whole body images of the animals were acquired in dynamic mode (for 15 min with 1 min
42
43 interval) and at 5, 60, 120, 180 min and 24 h post-injection by use of large field-of-view dual-
44
45 head gamma camera (Infinia Hawkeye®, GE Healthcare, Milwaukee, USA) fitted with a high
46
47 resolution and high energy collimator. The images were acquired from anterior, posterior, left
48
49 lateral, right lateral, dorsal and ventral views. After re-anesthetization at 180 min and 24 h post-
50
51 injection the animals were sacrificed and organs of interest and remaining carcass were collected,
52
53 weighed and counted for the radioactivity in a well-type Beckman 8000 gamma counter
54
55
56
57
58 (Beckman, Brea, CA). Approximately 75% of the total blood volume was withdrawn by cardiac
59
60
61
62
63
64
65

1
2
3
4 puncture and counted for radioactivity. The radioactivity in the sample and an aliquot of the
5
6 injection mixture was determined and reported as % injected dose g^{-1} of the tissue.
7
8
9

10 11 **Biodistribution After Oral Administration of $^{198}\text{AuNPs}$ in Rabbit**

12
13
14

15
16 A suspension of AX-encapsulated $^{198}\text{AuNPs}$ containing $20.0 \mu\text{g mL}^{-1}$ Au having $\sim 1200 \mu\text{Ci mL}^{-1}$
17
18 activity in saline (2.00 mL) adjusted to pH 7 was administered orally to the rabbits (n=4). The
19
20 animals were anesthetized by intramuscular ketamine injection (50 mg kg^{-1}) and fixed on a
21
22 wooden board. A flexible cannula was placed in the upper third of the oesophagus and AX-
23
24 encapsulated $^{198}\text{AuNPs}$ suspension (2.0 mL) was gently instilled and images were recorded from
25
26 anterior, posterior, left lateral, right lateral, dorsal and ventral sides at 5 min, 0.5, 1, 2, 24, 48 and
27
28
29
30
31 96 h post-administration.
32
33
34
35

36 ***In vitro* Distribution of $^{198}\text{AuNPs}$ in Serum Proteins**

37
38
39
40

41 Serum samples (0.5 mL, n = 3) from healthy human were vortex-mixed with equal volumes of
42
43 AX-encapsulated $^{198}\text{AuNPs}$ equivalent to $14.0 \mu\text{g mL}^{-1}$ Au having $\sim 1000 \text{ mCi mL}^{-1}$ suspension
44
45 and a buffer mixture (Tris, 2 SDS, 10 % glycerol and 0.0125 % bromophenol blue; pH adjusted
46
47 to 6.8 with HCl or NaOH solution). The samples were incubated at 37°C for 1h and subjected to
48
49 SDS-polyacrylamide gel (SDS-PAGE) analysis at 50 mA/gel [41]. The gel was stained with a
50
51 staining solution coomassie brilliant blue R-250 in (water-methanol-glacial acetic acid,
52
53 50:10:0.25) for 10 min. The gel was de-stained in methanol-acetic acid-water solution
54
55
56
57
58
59
60
61
62
63
64
65

1
2
3
4 (250:100:650) until protein fractions appeared clear. The strips were dried for 2–3 min in air then
5
6
7 at 70 °C in an oven for 30 min. The bands were cut ($3 \times 1 \text{ mm}^2$) and counted for radioactivity.
8
9

10 11 12 **Hemocompatibility Study**

13
14
15
16
17 Hemocompatibility of AX-encapsulated $^{198}\text{AuNPs}$ was studied by direct exposure for 3 h of
18
19 fresh blood (0.5 mL) from healthy humans (n=4) to $^{198}\text{AuNPs}$ (0.2 mL) equivalent to $14.0 \mu\text{g mL}^{-1}$
20
21 ^{198}Au having $\sim 1000 \text{ mCi mL}^{-1}$ at 37 °C. Optical images were taken at 0, 5, 10, 30, 60 and 120 min
22
23
24 by Euromax iScope (Holland) microscope; AX mucilage was used as the control.
25
26
27

28 29 **Complement activation**

30
31
32
33
34
35 Complement fixation test was performed by turbidimetric method [42] by measuring the
36
37 depletion of complement protein C_3 on incubation with the AX suspension and AX-encapsulated
38
39 $^{198}\text{AuNPs}$ separately. The AX suspension (0.2 mL) and $^{198}\text{AuNPs}$ equivalent to $14.0 \mu\text{g mL}^{-1}$ of
40
41 Au were incubated for 1 h at 37°C with of citrated blood (0.2 mL). The final concentration of the
42
43 $^{198}\text{AuNPs}$ in the assay was adjusted to $7.0 \mu\text{g mL}^{-1}$. The assay was performed in triplicate
44
45
46 according to the protocol provided by the kit manufacturer.
47
48
49

50 51 **Statistical Analysis**

52
53
54 The data was analyzed by employing the student t-test and one way-ANOVA where appropriate
55
56 using Statgraphics® Centurion 18 (Statgraphics Technologies, Inc., USA) software with $p < 0.05$
57
58
59 significance level. The graphs were plotted by use of MS Excel® 2010.
60
61

Results and Discussion

AX from ispaghula is a well-established food ingredient and herbal remedy for bowel disorders. It is a well-characterized highly branched hemicellulosic material soluble in alkaline and insoluble in acidic media [43]. The AX used in the present work was found to be similar to the previously reported material [34] as revealed by elemental, monosaccharide, ATR-FT-IR and GPC analyses (Table 1). Other than ispaghula AX is found in a variety of cereals grains including rice, wheat, corn, rye, oat, barley and sorghum. It is also part of several plant cell walls such as bamboo and pangola grass [44]. It has a linear Xylp backbone, partially substituted with α -L-Araf residues on O-3 or O-2 or both of the Xylp units (Scheme 1) [45]. It is composed of arabinose and xylose which are reducing sugars. The monosaccharides are released on partial hydrolysis of the polysaccharide in acidic environment provided by the gold salt, $\text{H}^{198}\text{AuCl}_4 \cdot 3\text{H}_2\text{O}$, in the present work. The cyclic structure of the monosaccharides is known to exist in equilibrium with the aldose form that affords reduction of Au^{3+} to Au^0 in the reaction mixture. This process is outlined in Scheme 1.

Our previous experience with AX for synthesis of non-radioactive AuNPs [29] prompted us to use this material for synthesis of ^{198}Au NPs. Among 36 radioisotopes of gold ^{198}Au is the most common isotope used for diagnosis and radiotherapy due to its appropriate half-life of 2.7 days [22]. Therefore, we attempted to synthesize ^{198}Au NPs using AX as reducing and capping agent for diagnostic imaging.

Synthesis and Characterization of ^{198}Au NPs

1
2
3
4
5
6
7 The $^{198}\text{AuNPs}$ were successfully prepared according to the method described in Materials and
8
9 Methods section. It was observed that AX reduced gold ions to NPs within 25 min at 50°C . The
10
11 optimal time and temperature were determined through preliminary experiments. The reduction
12
13 process was witnessed by colour changes from yellow to purple and finally to ruby red. The
14
15 reaction was monitored by recording the SPR spectra in the 350-800 nm range (Fig. 1a). The
16
17 position of the absorption band at 526 nm indicates that the particles are spherical in shape having
18
19 an average size of 30 nm [37]. The optimum conditions to obtain the SPR band at 526 nm were:
20
21 amount of mucilage (0.1 %) 16 mL/40 mL, amount of $\text{H}^{198}\text{AuCl}_4$ (0.1 mM) 20 mL/40 mL, pH 8,
22
23 time 25 min and temperature 50°C .
24
25
26
27
28

29 The XRD spectra (Fig. 1b) revealed characteristic face-centered cubic phase (JCPDS File
30
31 No. 87-0720). The peaks were assigned to (1 1 1), (2 0 0), (2 2 2) and (3 1 1) planes of the
32
33 nanocrystalloids. The intensities of the peaks suggest that the NPs were mainly oriented along (1
34
35 1 1) plane. The average size ($n = 3$) of the particles calculated from the XRD spectra by use of
36
37 Debye–Scherrer equation were found to be 28 ± 3 nm. The TEM image (Fig. 1c) revealed that the
38
39 particles were spherical in shape with size range of 25–30 nm. The DLS analysis provides
40
41 information about hydrodynamic diameter and polydispersity index (PDI) of NPs. The
42
43 hydrodynamic diameter thus determined was 101.4 ± 1.2 at pH 8. The relatively larger diameter
44
45 by DLS indicates that the particles were covered with the AX film which swell on contact with
46
47 the buffer solution [46]. The ζ value -23.5 ± 3.2 indicated that the particles should be stable for a
48
49 couple of months [47]. However, the particles synthesized by use of AX in the present work
50
51 exhibited exceptional stability extending over three years, which suggests that the AX plays a role
52
53
54
55
56
57
58
59
60
61
62
63
64
65

1
2
3
4 in imparting exceptional stability to the particles. The PDI value of 0.322 reveals a narrow size
5
6
7 distribution (Fig. 1d).
8
9

10 11 **Cell Viability and Cytotoxicity Study** 12 13

14
15
16 Biocompatibility of the AX-encapsulated $^{198}\text{AuNPs}$ was assessed by the NR uptake assay that
17
18 provided a quantitative estimation of the number of viable cells in the culture. It is one of the
19
20 widely used tests for the purpose [39]. It was found that incubation of HeLa cells with AX, AX-
21
22 encapsulated $^{198}\text{AuNPs}$ at different concentrations and $^{198}\text{AuNPs}$ and did not affect the viability
23
24 and morphology of the cells significantly (Fig. 2a-d) indicating their non-toxic nature. Thus, the
25
26 AX-encapsulated $^{198}\text{AuNPs}$ can be used for *in vivo* diagnostic studies.
27
28
29

30
31 In order to rule out the interference of $^{198}\text{AuNPs}$ with neutral red assay a secondary
32
33 cytotoxicity test was performed by potato disc assay. In this assay the tumour was induced by *A.*
34
35 *tumefaciens*, which is considered histologically similar to that in animals and humans [40, 48] A
36
37 negligible inhibition i.e., < 5 % was observed (Fig. 2e) suggesting the non-toxic nature of
38
39 particles.
40
41
42
43
44
45

46 **Biodistribution After Intravenous Administration of $^{198}\text{AuNPs}$ in Rabbit** 47 48 49

50
51 In order to validate the *in vivo* study, stability of the AX-encapsulated $^{198}\text{AuNPs}$ was checked *in*
52
53 *vitro* in biologically relevant media [49] including 10% NaCl, 0.2M cysteine, 0.2M histidine and
54
55 0.2M HSA at physiological pH for the time required to complete the study, i.e. 60 h. Typical
56
57 spectra in HSA on time scale are shown in Fig. 3b. The AX-encapsulated $^{198}\text{AuNPs}$ suspensions
58
59
60

1
2
3
4 were found to be stable in all these media for that time. It was observed that there was no
5
6 appearance of the band around 320 nm, characteristic of Au³⁺ compounds [50]. This clearly
7
8 suggests that the particles do not ionize in the period under investigation.
9

10
11 Biodistribution data and gamma-camera images obtained after i.v. administration of
12
13 AX-encapsulated¹⁹⁸AuNPs at fixed intervals of time are exhibited in Fig. 4. Highest uptake of
14
15 ¹⁹⁸AuNPs after 3 h, was found in the spleen followed by liver, heart, muscle, kidneys and lungs
16
17 (Fig. 4a). After 24 h the activity was not detectable in spleen and was significantly higher in
18
19 liver.
20
21
22
23
24
25

26 **Biodistribution After Oral Administration of ¹⁹⁸AuNPs in Rabbit**

27
28
29
30

31 The gamma-camera images obtained after oral administration of AX-encapsulated ¹⁹⁸AuNPs are
32
33 shown in Fig. 5. It can be seen that the activity did not move from stomach even after 24 h. This
34
35 means that the particles are firmly encapsulated by AX, which coagulated there being insoluble
36
37 in acidic medium. This effect was verified when the activity moved on oral administration of 1%
38
39 sodium bicarbonate solution (5 mL) and accumulated in colon and remained confined there up to
40
41 last observation at 96 h. These results suggest that the AX-encapsulated ¹⁹⁸AuNPs may be used
42
43 for a drug delivery at colon or as diagnostic probes. At colon there is a host of enzymes including
44
45 glycosidases and xylosidases, which would hydrolyse AX [51] in addition to a basic pH there.
46
47 Thus, this study presents AX as a highly biocompatible capping agent for AuNPs for their use in
48
49 medicine. A problem associated with other colon-specific drug delivery systems [52] is that a
50
51 major drug loss occurs before they reach the ileocecal junction.
52
53
54
55
56
57
58
59
60
61
62
63
64
65

***In vitro* Distribution of ¹⁹⁸AuNPs in Serum Proteins**

Five proteins bands separated after incubation of healthy human serum with AX-encapsulated ¹⁹⁸AuNPs are shown in Fig. 6 and distribution of radioactivity in these bands is depicted as bar graph (Fig. 6). The highest affinity of gold was recorded for α_1 -globulin (6.5%) followed by α_2 -globulin (~2%), β -globulin (~1%), γ -globulin (0.707%) and albumin (0.66%). Binding of gold with globulins from auranofin, an oral gold drug for rheumatoid arthritis, has also been reported previously [53, 54]. These results suggest that globulins can be labelled with radioactive gold by use of AX-ecapsulated¹⁹⁸AuNPs. Globulins play important role in inflammatory and malignancy processes. Therefore, the ¹⁹⁸Au-labelled globulins may find some useful applications as diagnostics and therapeutics.

Hemocompatibility Study

This study was carried out to assess the morphological effects of AX-encapsulated¹⁹⁸AuNPs on blood cells. No haemolysis was observed, whereas rouleaux effect (Fig. 7) was there with AX without NPs. The rouleaux effect is commonly observed with polysaccharides and polyols [55] and is not a deleterious effect. Mechanism of such type of aggregation of erythrocytes is not yet fully understood.

Complement activation

1
2
3
4 The amount of C₃ in blood before incubation was 128 %. After incubation with AX and
5
6 ¹⁹⁸AuNPs separately, the amount of C₃ was 125 ± 6.35 % and 129 ± 5.14 %, respectively. These
7
8 results clearly indicate that AX and ¹⁹⁸AuNPs do not activate the complement system. Thus the
9
10 AX-encapsulated ¹⁹⁸AuNPs appear to be biocompatible [50].
11
12
13
14
15
16

17 **Conclusions**

18
19
20
21

22 This study demonstrates that ¹⁹⁸AuNPs synthesized by use of AX (a food material) as the
23
24 reducing and dispersing agent are non-toxic to HeLa cells and *A. tumefaciens* and biocompatible.
25
26 The AX-encapsulated ¹⁹⁸AuNPs exhibited different biodistribution *in vivo* depending upon the
27
28 route of administration. After oral administration they accumulated at colon in rabbit after passing
29
30 through stomach and produced good quality gamma images. After i. v. administration to rabbit
31
32 and mouse they accumulated in liver. Thus, the AX-encapsulated ¹⁹⁸AuNPs appear to have
33
34 potential for use as diagnostic and therapeutic agents. Since ¹⁹⁸Au is both γ and β emitter, these
35
36 particles show a promise for use in image-guided nanoparticle therapies of cancer and advanced
37
38 drug delivery devices. In diagnostics gamma imaging is preferred because of its lower limit of
39
40 detection as compared to other techniques. These properties have been imparted to the particles
41
42 by the presence of AX.
43
44
45
46
47
48
49
50
51
52
53

54 **Compliance with Ethical Standards**

55
56
57
58

59 **Conflict of Interest** The authors declare that there is no conflict of interest.
60
61
62
63
64
65

1
2
3
4
5
6
7 **Ethical Approval for use of human blood and animals** The study protocols regarding use of
8
9 human blood and animals were reviewed and approved by Institutional Review Board of Forman
10
11 Christian College Lahore. Written informed consent was obtained from the blood donors (healthy
12
13 human adults). Guidelines provided in Good Clinical Practice by ICH, World Medical
14
15 Association Declaration of Helsinki and APA Committee on Animal Research and Ethics
16
17 (CARE), USA were followed.
18
19
20
21
22

23 **References**

- 24
25
26
27
28
29 1. Riley RS, Day ES (2017) Gold nanoparticle-mediated photothermal therapy: applications
30
31 and opportunities for multimodal cancer treatment. *Wiley Interdiscip Rev Nanomed*
32
33 *Nanobiotech* 9
- 34
35
36
37 2. Mahan MM, Doiron AL (2018) Gold Nanoparticles as X-Ray, CT, and Multimodal
38
39 Imaging Contrast Agents: Formulation, Targeting, and Methodology. *J Nanomater*
40
41 2018:1–15
- 42
43
44 3. Ruan S, Yuan M, Zhang L, et al (2015) Tumor microenvironment sensitive doxorubicin
45
46 delivery and release to glioma using angiopep-2 decorated gold nanoparticles.
47
48 *Biomaterials* 37:425–435. <https://doi.org/10.1016/J.Biomaterials.2014.10.007>
- 49
50
51 4. Manohar N, Reynoso FJ, Diagaradjane P, et al (2016) Quantitative imaging of gold
52
53 nanoparticle distribution in a tumor-bearing mouse using benchtop x-ray fluorescence
54
55 computed tomography. *Sci Rep* 6:22079. <https://doi.org/10.1038/srep22079>
- 56
57
58 5. Vigderman L, Zubarev ER (2013) Therapeutic platforms based on gold nanoparticles and
59
60

1
2
3
4 their covalent conjugates with drug molecules. *Adv Drug Deliv Rev* 65:663–676.

5
6
7 <https://doi.org/10.1016/j.addr.2012.05.004>

- 8
9 6. Jain PK (2014) *Gold Nanoparticles for Physics, Chemistry and Biology*. Edited by
10 Catherine Louis and Olivier Pluchery. *Angew Chemie Int Ed* 53:1197–1197.
11
12 <https://doi.org/10.1002/anie.201309807>
13
14
15 7. Nam J-M, Thaxton CS, Mirkin CA, et al (2009) *Gold Nanoparticles : Assembly ,*
16
17
18 *Supramolecular Chemistry , Quantum-Size-Related Properties , and Applications toward*
19
20 *Biology , Catalysis , and Nanotechnology*. *Nature* 9:1–8.
21
22 <https://doi.org/10.1016/j.toxlet.2005.10.003>
23
24
25 8. Her S, Jaffray DA, Allen C (2017) *Gold nanoparticles for applications in cancer*
26
27
28 *radiotherapy: Mechanisms and recent advancements*. *Adv Drug Deliv Rev* 109:84–101
29
30
31 9. Austin LA, MacKey MA, Dreaden EC, El-Sayed MA (2014) *The optical, photothermal,*
32
33
34 *and facile surface chemical properties of gold and silver nanoparticles in biodiagnostics,*
35
36 *therapy, and drug delivery*. *Arch Toxicol* 88:1391–1417
37
38 10. Qu X, Li Y, Li L, et al (2015) *Fluorescent Gold Nanoclusters : Synthesis and Recent*
39
40
41 *Biological Application*. *J Nanomater* 2015:Article ID 784097
42
43 11. Ma Z, Xia H, Liu Y, et al (2013) *Applications of gold nanorods in biomedical imaging*
44
45
46 *and related fields*. *Chinese Sci Bull* 58:2530–2536. [https://doi.org/10.1007/s11434-013-](https://doi.org/10.1007/s11434-013-5720-7)
47
48 [5720-7](https://doi.org/10.1007/s11434-013-5720-7)
49
50 12. Jain PK, Lee KS, El-Sayed IH, El-Sayed MA (2006) *Calculated absorption and scattering*
51
52
53 *properties of gold nanoparticles of different size, shape, and composition: Applications in*
54
55
56 *biological imaging and biomedicine*. *J Phys Chem B* 110:7238–7248.
57
58 <https://doi.org/10.1021/jp057170o>
59
60
61
62
63
64
65

- 1
2
3
4
5
6
7
8
9
10
11
12
13
14
15
16
17
18
19
20
21
22
23
24
25
26
27
28
29
30
31
32
33
34
35
36
37
38
39
40
41
42
43
44
45
46
47
48
49
50
51
52
53
54
55
56
57
58
59
60
61
62
63
64
65
13. Liu X, Atwater M, Wang J, Huo Q (2007) Extinction coefficient of gold nanoparticles with different sizes and different capping ligands. *Colloids Surfaces B Biointerfaces* 58:3–7. <https://doi.org/10.1016/j.colsurfb.2006.08.005>
 14. Alric C, Taleb J, Le Duc G, et al (2008) Contrast Agents for Both X-ray Computed Tomography and Magnetic Resonance Imaging. *J Am Chem Soc* 130:5908–5915. <https://doi.org/10.1021/ja078176p>
 15. Norouzi H, Khoshgard K, Akbarzadeh F (2018) In vitro outlook of gold nanoparticles in photo-thermal therapy: a literature review. *Lasers Med Sci* 33:917–926
 16. Huang X, El-Sayed MA (2011) Plasmonic photo-thermal therapy (PPTT). *Alexandria J Med* 47:1–9. <https://doi.org/10.1016/j.ajme.2011.01.001>
 17. Axiak-Bechtel SM, Upendran A, Lattimer JC, et al (2014) Gum arabic-coated radioactive gold nanoparticles cause no short-term local or systemic toxicity in the clinically relevant canine model of prostate cancer. *Int J Nanomedicine* 9:5001–11. <https://doi.org/10.2147/IJN.S67333>
 18. Shukla R, Chanda N, Zambre A, et al (2012) Laminin receptor specific therapeutic gold nanoparticles (198AuNP-EGCg) show efficacy in treating prostate cancer. *Proc Natl Acad Sci* 109:12426–12431. <https://doi.org/10.1073/pnas.1121174109>
 19. Chanda N, Kan P, Watkinson LD, et al (2010) Radioactive gold nanoparticles in cancer therapy: therapeutic efficacy studies of GA-198AuNP nanoconstruct in prostate tumor-bearing mice. *Nanomedicine Nanotechnology, Biol Med* 6:201–209. <https://doi.org/10.1016/j.nano.2009.11.001>
 20. Radionuclide NR-, Phillips WT, Otto RA, Bao A (2011) Interventional Therapy of Head and Neck Cancer with Lipid Nanoparticle-Carried Rhenium-186 Radionuclide. *J Vasc*

- 1
2
3
4 Interv Radiol 21:1271–1279. <https://doi.org/10.1016/j.jvir.2010.02.027>. Interventional
5
6
7 21. Al-Yasiri AY, Khoobchandani M, Cutler CS, et al (2017) Mangiferin functionalized
8
9 radioactive gold nanoparticles (MGF- 198 AuNPs) in prostate tumor therapy: green
10
11 nanotechnology for production, in vivo tumor retention and evaluation of therapeutic
12
13 efficacy. *Dalt Trans* 46:14561–14571. <https://doi.org/10.1039/C7DT00383H>
14
15
16 22. Tobias JS, Hochhauser D (2009) *Cancer and its Management*. John Wiley & Sons
17
18
19 23. Kim D, Park S, Jae HL, et al (2007) Antibiofouling polymer-coated gold nanoparticles as
20
21 a contrast agent for in vivo X-ray computed tomography imaging. *J Am Chem Soc*
22
23 129:7661–7665. <https://doi.org/10.1021/ja071471p>
24
25
26 24. Lee J, Chatterjee DK, Lee MH, Krishnan S (2014) Gold nanoparticles in breast cancer
27
28 treatment: Promise and potential pitfalls. *Cancer Lett* 347:46–53
29
30
31 25. Hainfeld JF, Slatkin DN, Smilowitz HM (2004) The use of gold nanoparticles to enhance
32
33 radiotherapy in mice. *Phys Med Biol* 49:. <https://doi.org/10.1088/0031-9155/49/18/N03>
34
35
36 26. Chen Y, Wang X (2008) Novel phase-transfer preparation of monodisperse silver and
37
38 gold nanoparticles at room temperature. *Mater Lett* 62:2215–2218.
39
40
41 <https://doi.org/10.1016/j.matlet.2007.11.050>
42
43
44 27. Jeong GH, Lee YW, Kim M, Han SW (2009) High-yield synthesis of multi-branched gold
45
46 nanoparticles and their surface-enhanced Raman scattering properties. *J Colloid Interface*
47
48 *Sci* 329:97–102. <https://doi.org/10.1016/J.JCIS.2008.10.004>
49
50
51 28. Deraedt C, Salmon L, Gatard S, et al (2014) Sodium borohydride stabilizes very active
52
53 gold nanoparticle catalysts. *Chem Commun* 50:14194–14196.
54
55
56 <https://doi.org/10.1039/c4cc05946h>
57
58
59 29. Amin M, Iram F, Iqbal MS, et al (2013) Arabinoxylan-mediated synthesis of gold and
60
61
62
63
64
65

- 1
2
3
4 silver nanoparticles having exceptional high stability. *Carbohydr Polym* 92:1896–900.
5
6 <https://doi.org/10.1016/j.carbpol.2012.11.056>
7
8
- 9 30. Iram F, Iqbal MS, Athar MM, et al (2014) Glucoxylyan-mediated green synthesis of gold
10 and silver nanoparticles and their phyto-toxicity study. *Carbohydr Polym* 104:29–33.
11
12 <https://doi.org/10.1016/j.carbpol.2014.01.002>
13
14
- 15 31. Rabito MF, Reis AV, Reis Freitas A dos, et al (2012) A pH/enzyme-responsive polymer
16 film consisting of Eudragit® FS 30 D and arabinoxylane as a potential material
17
18 formulation for colon-specific drug delivery system. *Pharm Dev Technol* 17:429–436.
19
20 <https://doi.org/10.3109/10837450.2010.546409>
21
22
- 23 32. Agarwal VK, Gupta A, Chaturvedi S, Khan F (2016) Polysaccharide: Carrier in colon
24 targeted drug delivery system. *MIT Int J Pharm Sci* 2:1–9
25
26
- 27 33. Lemarchand C, Gref R, Couvreur P (2004) Polysaccharide-decorated nanoparticles. *Eur J*
28
29 *Pharm Biopharm* 58:327–341
30
31
- 32 34. Massey S, Iqbal MS, Wolf B, et al (2016) Comparative drug loading and release study on
33 some carbohydrate polymers. *Lat Am J Pharm* 35:146–155
34
35
- 36 35. Weitzhandler M, Barreto V, Pohl C, et al (2004) CarboPac™ PA20: A new
37 monosaccharide separator column with electrochemical detection with disposable gold
38
39 electrodes. *J Biochem Biophys Methods* 60:309–317.
40
41 <https://doi.org/10.1016/j.jbbm.2004.01.009>
42
43
- 44 36. Saeman JF, Moore WE, Mitchell RL, Millett MA (1954) Techniques for the determination
45 of pulp constituents by quantitative paper chromatography. *Tappi J* 37:336–343
46
47
- 48 37. Rahman S (2016) Size and Concentration Analysis of Gold Nanoparticles With
49 Ultraviolet-Visible Spectroscopy. *Undergrad J Math Model One + Two* 7:13.
50
51
52
53
54
55
56
57
58
59
60
61
62
63
64
65

- 1
2
3
4 <https://doi.org/http://dx.doi.org/10.5038/2326-3652.7.1.4872>
5
6
7 38. Scherrer P Bestimmung der Größe und der inneren Struktur von Kolloidteilchen mittels
8 Röntgenstrahlen. Nachrichten von der Gesellschaft der Wissenschaften zu Göttingen,
9 Math Klasse 1918:98–100
10
11
12
13
14 39. Repetto G, del Peso A, Zurita JL (2008) Neutral red uptake assay for the estimation of cell
15 viability/cytotoxicity. Nat Protoc 3:1125–31. <https://doi.org/10.1038/nprot.2008.75>
16
17
18
19 40. Trigui F, Pigeon P, Jalleli K, et al (2013) Selection of a suitable disc bioassay for the
20 screening of anti-tumor molecules. Int J Biomed Sci 9:230–6
21
22
23
24 41. Laemmli UK (1970) Cleavage of structural proteins during the assembly of the head of
25 bacteriophage T4. Nature 227:680–5
26
27
28
29 42. Parker AR, Jolles S, Ponsford M, et al (2018) Quantification of human C1 esterase
30 inhibitor protein using an automated turbidimetric immunoassay. J Clin Lab Anal
31 33:e22627. <https://doi.org/10.1002/jcla.22627>
32
33
34
35
36 43. Saghir S, Iqbal MS, Hussain MA, et al (2008) Structure characterization and
37 carboxymethylation of arabinoxylan isolated from Ispaghula (*Plantago ovata*) seed husk.
38 Carbohydr Polym 74:309–317. <https://doi.org/10.1016/j.carbpol.2008.02.019>
39
40
41
42
43 44. Biliaderis C, Izydorczyk M (2007) Functional Food Carbohydrates
44
45
46 45. Iram F, Massey S, Iqbal MS, Ward DG (2018) Structural investigation of hemicelluloses
47 from *Plantago ovata*, *Mimosa pudica* and *Lallemantia royleana* by MALDI-ToF mass
48 spectrometry. J Carbohydr Chem 37:1–17.
49 <https://doi.org/10.1080/07328303.2018.1487973>
50
51
52
53
54
55 46. Tomaszewska E, Soliwoda K, Kadziola K, et al (2013) Detection Limits of DLS and UV-
56 Vis Spectroscopy in Characterization of Polydisperse Nanoparticles Colloids. J
57
58
59
60
61
62
63
64
65

- 1
2
3
4 Nanomater 2013:60:60--60:60. <https://doi.org/10.1155/2013/313081>
- 5
6
7 47. Bhattacharjee S (2016) DLS and zeta potential - What they are and what they are not? J
8
9 Control Release 235:337–351
- 10
11 48. Smith EF (1916) Studies on the crown gall of plants its relation to human cancer. J Cancer
12
13 Res 1:231–309. <https://doi.org/10.1158/jcr.1916.231>
- 14
15
16 49. Kattumuri V, Katti K, Bhaskaran S, et al (2007) Gum arabic as a phytochemical construct
17
18 for the stabilization of gold nanoparticles: In vivo pharmacokinetics and X-ray-contrast-
19
20 imaging studies. Small 3:333–341. <https://doi.org/10.1002/sml.200600427>
- 21
22
23 50. Brown DH, McKinlay GC, Smith WE (1979) The electronic spectra of some gold(III)
24
25 complexes. Inorganica Chim Acta 32:117–121. <https://doi.org/10.1016/S0020->
26
27 1693(00)91648-7
- 28
29
30 51. Swarbrick J (1996) Encyclopedia of pharmaceutical technology. Pharm Technol 3:2004–
31
32 2020. <https://doi.org/10.1081/E-EPT-100001065>
- 33
34
35 52. Philip A, Philip B (2010) Colon Targeted Drug Delivery Systems: A Review on Primary
36
37 and Novel Approaches. Oman Med J 25:70–78. <https://doi.org/10.5001/omj.2010.24>
- 38
39
40 53. Iqbal MS, Taqi SG, Arif M, et al (2009) In vitro distribution of gold in serum proteins
41
42 after incubation of sodium aurothiomalate and auranofin with human blood and its
43
44 pharmacological significance. Biol Trace Elem Res 130:204–209.
45
46 <https://doi.org/10.1007/s12011-009-8330-0>
- 47
48
49 54. Israel L, Edelstein R, Mannoni P, et al (1977) Plasmapheresis in patients with
50
51 disseminated cancer: Clinical results and correlation with changes in serum protein. The
52
53 concept of “nonspecific blocking factors.” Cancer 40:3146–3154.
54
55 [https://doi.org/10.1002/1097-0142\(197712\)40:6<3146::AID-](https://doi.org/10.1002/1097-0142(197712)40:6<3146::AID-)
56
57
58
59
60
61
62
63
64
65

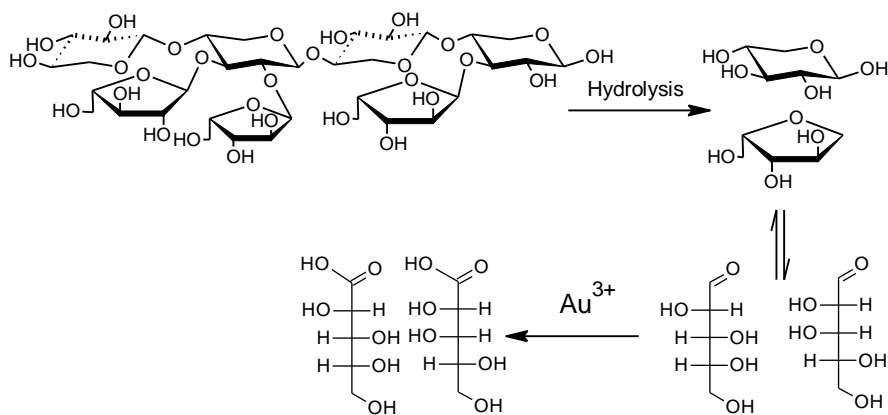
1
2
3
4
5
6
7
8
9
10
11
12
13
14
15
16
17
18
19
20
21
22
23
24
25
26
27
28
29
30
31
32
33
34
35
36
37
38
39
40
41
42
43
44
45
46
47
48
49
50
51
52
53
54
55
56
57
58
59
60
61
62
63
64
65

CNCR2820400659>3.0.CO;2-N

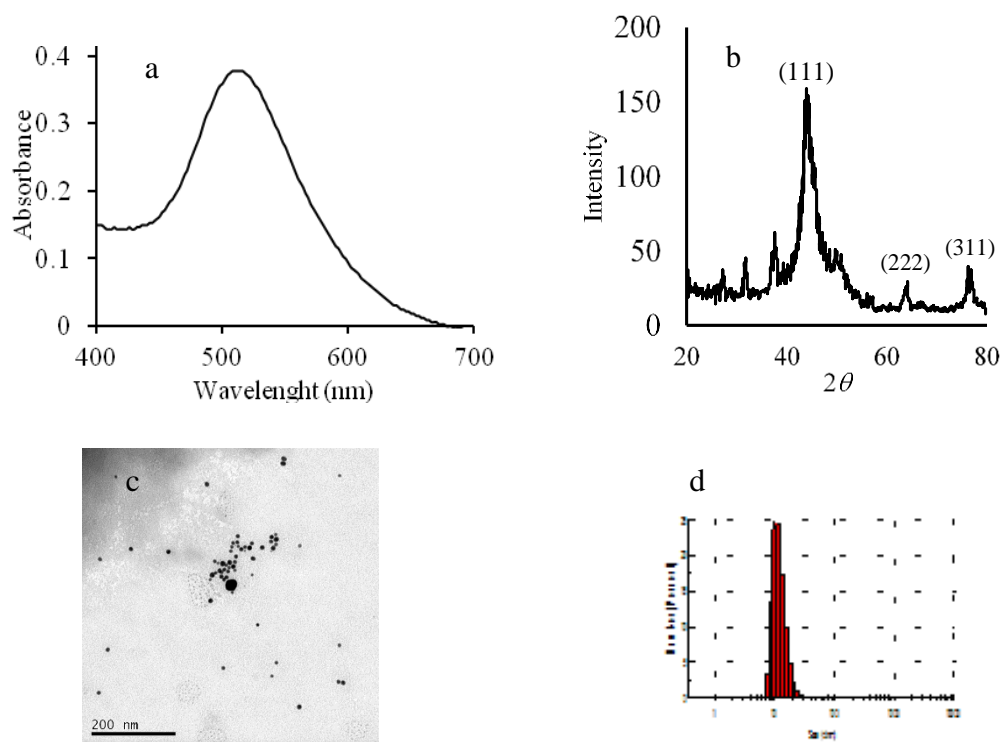
55. Robyt JF (1998) Essentials of Carbohydrate Chemistry. Springer Science & Business

Media

Figures



19 **Scheme 1** AX undergoing partial hydrolysis followed by ring opening and oxidation by Au³⁺.



48 **Fig. 1** Characterization of ¹⁹⁸AuNPs in AX (a) SPR spectrum (b) Powder XRD pattern of
49 ¹⁹⁸AuNPs (c) TEM images (d). Histogram of size distribution ¹⁹⁸AuNPs measured by DLS
50
51
52
53
54
55
56
57
58
59
60
61
62
63
64
65

technique.

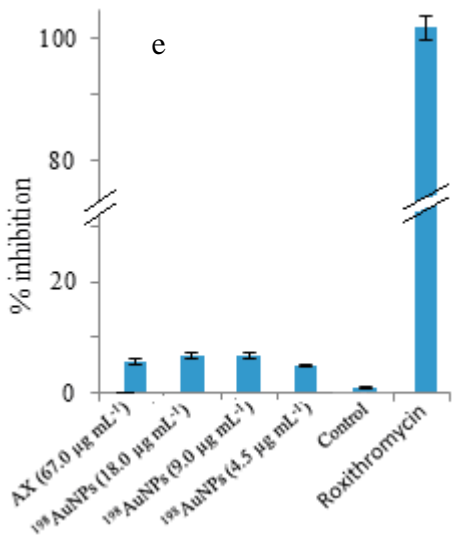
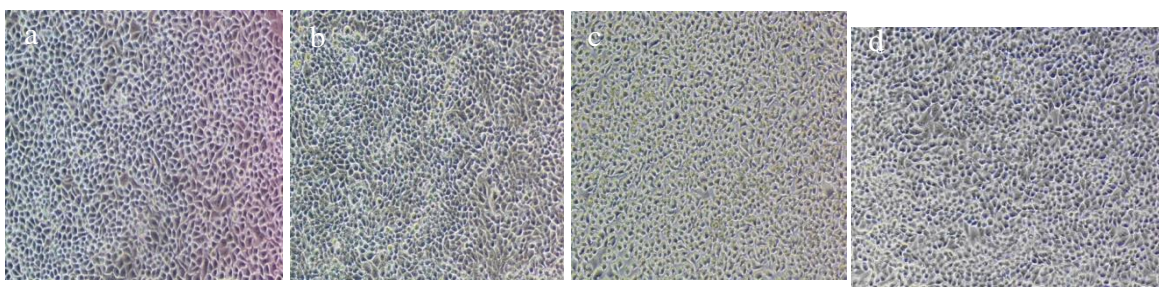
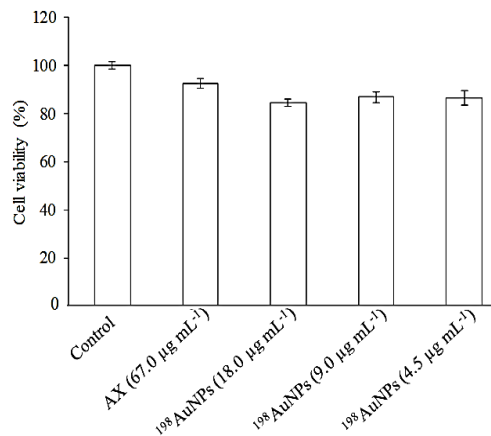
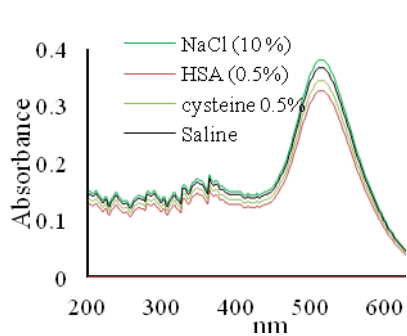
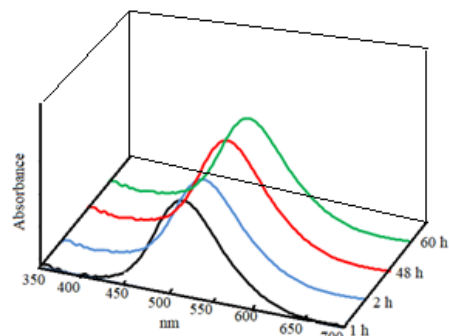


Fig 2 Top: Histogram showing % cell viability against HeLa cell line after incubation with AX suspension; Bottom: (a) microscopic images of the control cells (b) AX-treated cells and (c) AX-encapsulated ¹⁹⁸AuNPs-treated cells (d) ¹⁹⁸AuNPs-treated cells showing no morphological changes, (e) Histogram showing % inhibition of *A. tumefaciens* by AX-encapsulated ¹⁹⁸AuNPs and roxithromycin used as positive control in potato disc assay. The results are expressed as the mean ± SD (n = 6, p < 0.05, the error bars represent SD)

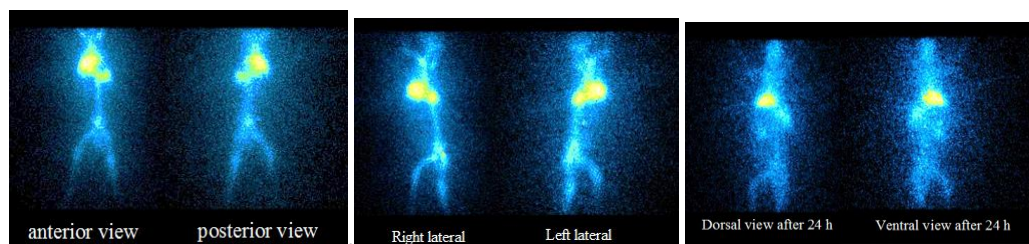
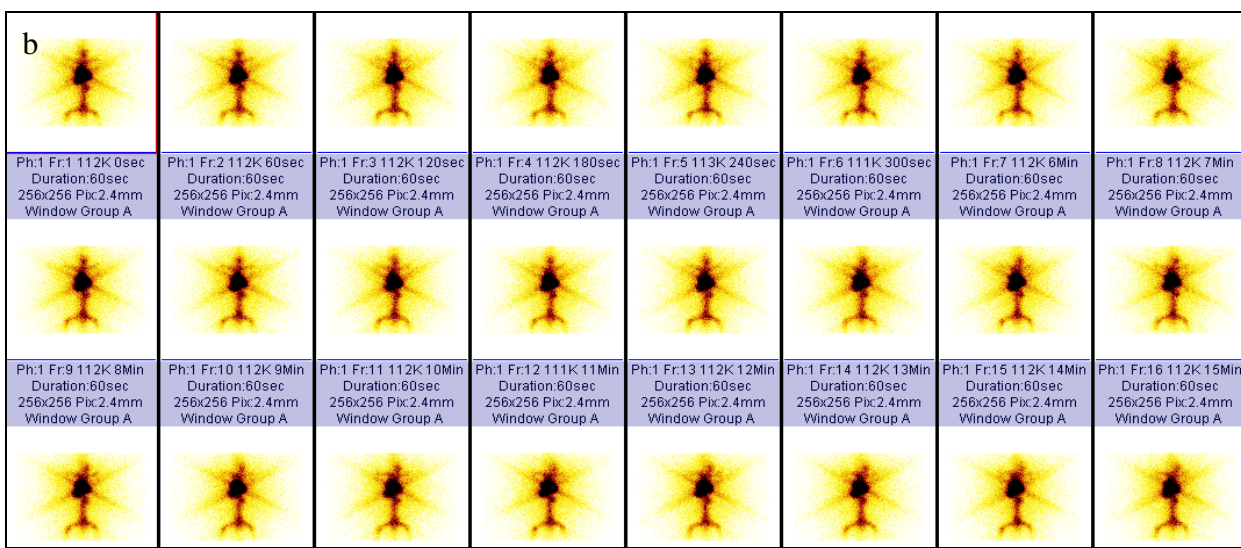
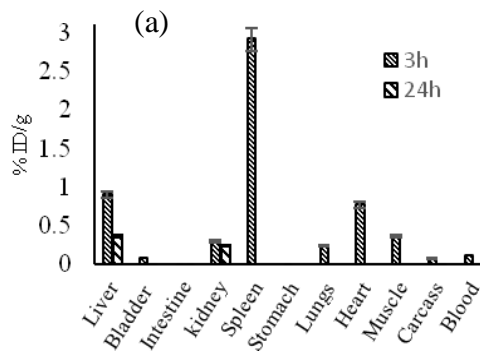


(a)



(b)

Fig 3 (a) Spectra showing stability (absence of 320-nm band) of AX-encapsulated $^{198}\text{AuNPs}$ in different media, (b) The SPR spectra of AX-encapsulated $^{198}\text{AuNPs}$ in 0.2 M HSA showing no significant shift in wavelength and absorbance with time.



(c)

Fig 4 (a) Biodistribution of ¹⁹⁸AuNPs (equivalent to 14.0 $\mu\text{g mL}^{-1}$ Au, activity $\sim 1000 \mu\text{Ci mL}^{-1}$. The rabbits were anesthetized by 50 mg kg^{-1} intramuscular ketamine injection) before administration of the dose) in various organs at 3 h and 24 h after i.v. administration; the amount of gold is expressed as a percentage of injected dose per gram (% ID g^{-1}) of organ/tissue. The results are expressed as the mean \pm SD ($n = 4$, $p < 0.05$, the error bars represent SD). (b) Dynamic gamma-camera images up to 15 min post i.v. injection (pH 7; 14.0 $\mu\text{g mL}^{-1}$; 1000 $\mu\text{Ci mL}^{-1}$). (c) Gamma-camera images of whole body (anterior, posterior, right lateral and left lateral views) at 180 min post-injection, dorsal at 24 h and ventral at 24 h, showing accumulation of radioactivity in liver and spleen, with negligible amount in other organs.

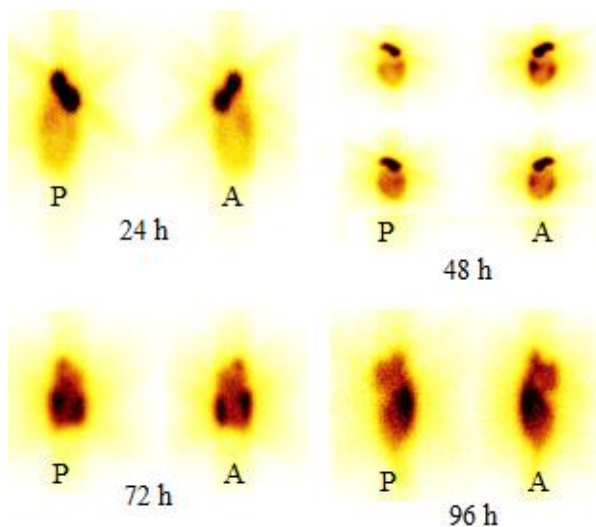


Fig 5 Gamma-camera images exhibiting accumulation of radioactivity at colon after oral administration of AX-¹⁹⁸AuNP (equivalent to 20.0 μg mL⁻¹ Au, activity ~1200 μCi mL⁻¹ in 2.0 mL saline adjusted to pH 7. The animals (n=4) were anesthetized by 50 mg kg⁻¹ intramuscular ketamine injection before administration) to rabbit in colon after 24, 48, 72 and 96 h. A: Anterior, P: posterior.

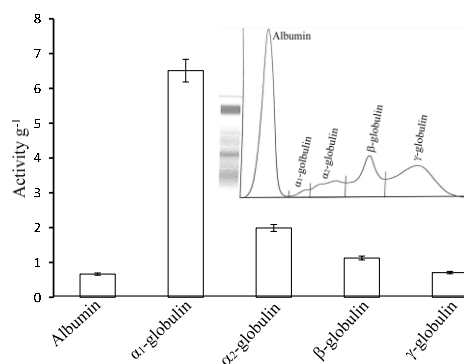


Fig 6 In-vitro distribution of AX-encapsulated¹⁹⁸AuNPs (equivalent to 14.0 μg mL⁻¹ Au, activity ~1000 mCi mL⁻¹) in serum proteins SDS-PAGE analysis; the results are expressed as the mean ± SD (n=4, p < 0.05, error bars represents SD). Inset shows separated protein bands.

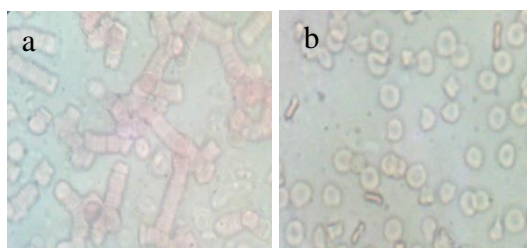


Fig 7 Optical images exhibiting rouleaux effect (a) AX treated-cells and (b) no effect by AX-encapsulated ¹⁹⁸AuNPs (200 μCi:500 μL) after 120 min.

1
2
3
4 **Table**
5
6

7 **Table 1** Analytical data of AX, Experimental (Literature [34, 43] for FT-IR).
8

9 CHN (%)	C 31.61 (31.59), H 4.59 (4.66), N 1.05 (1.20)
10 Monosaccharides (%)	Ara 23.24 (23.11), Xyl 76.67 (76.89), Uronic acids 1.3 (Not 11 determined)
12 Protein (%)	Not detectable (Not detectable)
13 Molar mass (g mol ⁻¹)	3.17×10 ⁶ (3.26×10 ⁶)
14 Moisture (%)	8.31 (8.24)
15 FT-IR bands (cm ⁻¹)	v(OH) 3417 (3414), v(CH) 2921 (2925), stretch due to absorbed 16 water merged with carboxylic group 1634 (1630), in-plane δ(OH) 17 1457 (1462), δ(CH ₂) 1423 (1417), δ(CH) 1367 (1375), antisym 18 bridge oxygen δ 1257,1152 (1249, 1162), δ(CO) 1041 (1043), ν _{sym} 19 (COC glycosidic linkage) 899 (896), polymer backbone vibrations 20 612, 531 (617,534) 21 22 23

Change of authorship request form (pre-acceptance)

Please read the important information on page 4 before you begin

This form should be used by authors to request any change in authorship including changes in corresponding authors. Please fully complete all sections. Use black ink and block capitals and provide each author's full name with the given name first followed by the family name.

Please note: In author collaborations where there is formal agreement for representing the collaboration, it is sufficient for the representative or legal guarantor (usually the corresponding author) to complete and sign the Authorship Change Form on behalf of all authors.

Section 1: Please provide the current title of manuscript

(For journals: Please provide the manuscript ID, title and/or DOI if available.)

(For books: Please provide the title, ISBN and/or DOI if available.)

Manuscript ID no. in case of unpublished manuscript: BTER-D-18-01156R3

DOI in case of published manuscript:

ISBN (for books):

Title: **Synthesis and Biodistribution Study of Biocompatible 198Au Nanoparticles by use of Arabinoxylan as Reducing and Stabilizing Agent**

Section 2: Please provide the previous authorship, in the order shown on the manuscript before the changes were introduced. Please indicate the corresponding author by adding (CA) behind the name.

	First name(s)	Family name	ORCID or SCOPUS id, if available
1 st author	Fozia (on manuscript); Mohammad S (in metadata)	Iram (on manuscript); Iqbal (in metadata)	
2 nd author	Fozia (in metadata); Mohammad S (on manuscript)	Iram (in metadata); Iqbal (on manuscript)	
3 rd author	Irfan Ullah	Khan	
4 th author	Rashid	Rasheed	
5 th author	Aqsa	Khalid	
6 th author	Muhammad	Khalid	
7 th author	Saira	Aftab	

Please use an additional sheet if there are more than 7 authors.

8th author Abdul R

Shakoori

Change of authorship request form (pre-acceptance)

Section 3: Please provide a justification for change. Please use this section to explain your reasons for changing the authorship of your manuscript, e.g. what necessitated the change in authorship? Please refer to the (journal) policy pages for more information about authorship. Please explain why omitted authors were not originally included and/or why authors were removed on the submitted manuscript.

There is no change of authorship on the manuscript; however the order of first two authors was reversed in metadata by mistake.

Section 4: Proposed new authorship. Please provide your new authorship list in the order you would like it to appear on the manuscript. Please indicate the corresponding author by adding (CA) behind the name. If the corresponding author has changed, please indicate the reason under section 3.

	First name(s)	Family name (this name will appear in full on the final publication and will be searchable in various abstract and indexing databases)
1 st author	Fozia	Iram
2 nd author	Mohamm S	Iqbal
3 rd author	Irfan Ullah	Kahan
4 th author	Rashid	Rasheed
5 th author	Aqsa	Khalid
6 th author	Muhammad	Khalid
7 th author	Saira	Aftab

Please use an additional sheet if there are more than 7 authors.



Change of authorship request form (pre-acceptance)

Section 5: Author contribution, Acknowledgement and Disclosures. Please use this section to provide a new disclosure statement and, if appropriate, acknowledge any contributors who have been removed as authors and ensure you state what contribution any new authors made (if applicable per the journal or book (series) policy). Please ensure these are updated in your manuscript - after approval of the change(s) - as our production department will not transfer the information in this form to your manuscript.

New acknowledgements:

No change

New Disclosures (financial and non-financial interests, funding):

No change

New Author Contributions statement (if applicable per the journal policy):









No change

State 'Not applicable' if there are no new authors.

Change of authorship request form (pre-acceptance)

Section 6: Declaration of agreement. All authors, unchanged, new and removed must sign this declaration.

(NB: Please print the form, sign and return a scanned copy. Please note that signatures that have been inserted as an image file are acceptable as long as it is handwritten. Typed names in the signature box are unacceptable.) * Please delete as appropriate. Delete all of the bold if you were on the original authorship list and are remaining as an author.

	First name	Family name	I agree to the proposed new authorship shown in section 4 /and the addition/removal* of my name to the authorship list.	Signature	Affiliated institute	Date
1 st author	Fozia	Iram	I agree to the proposed new authorship shown in section 4 /and the addition/removal* of my name to the authorship list.		Department of Chemistry, LCW University, Lahore	Mar 15, 2019
2 nd author	Mohammad S	Iqbal	I agree to the proposed new authorship shown in section 4 /and the addition/removal* of my name to the authorship list.		Department of Chemistry, Forman Christian College, Lahore	Mar 15, 2019
3 rd author	Irfan Ullah	Khan	I agree to the proposed new authorship shown in section 4 /and the addition/removal* of my name to the authorship list.		Radiopharmacy & PET Radiochemistry Division, Institute of Nuclear Medicine and Oncology, Lahore	Mar 15, 2019
4 th authors	Rashid	Rasheed	I agree to the proposed new authorship shown in section 4 /and the addition/removal* of my name to the authorship list.		Institute of Nuclear Medicine Oncology and Radiotherapy, Mansehra Road, Abbottabad	Mar 15, 2019
5 th author	Aqsa	Khalid	I agree to the proposed new authorship shown in section 4 /and the addition/removal* of my name to the authorship list.		Department of Chemistry, LCW University, Lahore	Mar 15, 2019
6 th author	Muhammad	Khalid	I agree to the proposed new authorship shown in section 4 /and the addition/removal* of my name to the authorship list.		Isotope Production Division, Pakistan Institute of Nuclear Science and Technology, PO Nilore, Islamabad	Mar 15, 2019
7 th author	Saira	Aftab	I agree to the proposed new authorship shown in section 4 /and the addition/removal* of my name to the authorship list.		School of Biological Sciences, University of the Punjab, Quaid-e-Azam Campus, Lahore	Mar 15, 2019
8 th author	Abdul R	Shakoori	I agree as above		School of Biological Sciences, University of the Punjab, Quaid-e-Azam Campus, Lahore	Mar 15, 2019

Please use an additional sheet if there are more than 7 authors.

SPRINGER NATURE Springer Nature is one of the world's leading global research, educational and professional publishers, created in May 2015 through the combination of Nature Publishing Group, Palgrave Macmillan, Macmillan Education and Springer Science+Business Media.

Change of authorship request form (pre-acceptance)

Important information. Please read.

- Please return this form, fully completed, to Springer Nature. We will consider the information you have provided to decide whether to approve the proposed change in authorship. We may choose to contact your institution for more information or undertake a further investigation, if appropriate, before making a final decision.
- By signing this declaration, all authors guarantee that the order of the authors are in accordance with their scientific contribution, if applicable as different conventions apply per discipline, and that only authors have been added who made a meaningful contribution to the work.
- Please note, we cannot investigate or mediate any authorship disputes. If you are unable to obtain agreement from all authors (including those who you wish to be removed) you must refer the matter to your institution(s) for investigation. Please inform us if you need to do this.
- If you are not able to return a fully completed form within **30 days** of the date that it was sent to the author requesting the change, we may have to withdraw your manuscript. We cannot publish manuscripts where authorship has not been agreed by all authors (including those who have been removed).
- Incomplete forms will be rejected.